

NORTHWESTERN UNIVERSITY

Surface Analysis of Superconducting Radiofrequency Cavities

A DISSERTATION

SUBMITTED TO THE GRADUATE SCHOOL  
IN PARTIAL FULFILLMENT OF THE REQUIREMENTS

for the degree

DOCTOR OF PHILOSOPHY

Field of Materials Science and Engineering

By

Eric Viklund

EVANSTON, ILLINOIS

October, 2024

## **Abstract**

## **Acknowledgements**

# Chapter 1

## Mechanical Polishing

### 1.1 Introduction

Superconducting radiofrequency (SRF) cavities are an essential component of particle accelerators used in various fields of science and industry, including high-energy physics, material science, and medical isotope production[1]. These cavities accelerate charged particles to very high energies and can achieve higher accelerating gradients at continuous operation than normal conducting cavities.

The performance of superconducting radio-frequency cavities is determined by the superconducting properties of the surface layer of the cavity. The low-temperature superconductor Nb<sub>3</sub>Sn has a higher superconducting transition temperature (T<sub>c</sub>), 18 K compared to 9 K, and a higher super-heating magnetic field (H<sub>sh</sub>), around 440 mT compared to 250 mT for the more commonly used niobium[2, 3, 4, 5]. SRF cavities coated with a layer of Nb<sub>3</sub>Sn can, therefore, achieve a much higher accelerating field, up to 100 MV/m in theory, and have a lower surface resistance than Nb SRF cavities at higher temperatures allowing for cavity operation at 4 K. Whereas Nb cavities are typically operated at 2 K e.g. the LCLS-II cryomodules[6]. These properties make Nb<sub>3</sub>Sn SRF cavities a promising research topic for future accelerators such as high-energy linacs or small-scale industrial accelerators.

Nb<sub>3</sub>Sn cavities are typically manufactured by coating a Nb cavity with a thin film of Nb<sub>3</sub>Sn using Sn vapor-diffusion[7, 8, 9], exposing a Nb cavity to tin vapor at 1,100 °C to create Nb<sub>3</sub>Sn. The reaction forms a 2-3 μm thick Nb<sub>3</sub>Sn film with grains approximately 1 μm large. The grains are faceted, and the grain boundaries are thermally etched resulting in approximately 100-150 nm of surface roughness.

Using the Sn vapor-diffusion coating technique[7, 8, 10], Nb<sub>3</sub>Sn cavities have only been able to reach a maximum accelerating gradient of 24 MV/m[11], a result that was achieved using a thinner Nb<sub>3</sub>Sn coating which is smoother than the typical coating. However, this result has not been reproducible, and the performance is lower than the theoretical maximum of Nb<sub>3</sub>Sn cavities.

Surface roughness is thought to be one of the limiting factors of Nb<sub>3</sub>Sn SRF cavity performance. Surface roughness has been shown to be a cause of Q slope and quench in niobium cavities treated with buffered chemical polishing (BCP) due to sharp grain boundary steps.[12, 13] Simulations of the magnetic field near a typical Nb<sub>3</sub>Sn surface show that the magnetic field is increased by up to 60 percent in some areas compared to a smooth surface[14, 15] and could be higher for particularly rough areas. By reducing the field enhancement caused by surface roughness, a corresponding increase in the cavity

accelerating gradient can be expected.

One method to achieve smoother Nb<sub>3</sub>Sn surfaces is polishing. Nb<sub>3</sub>Sn polishing has been a topic of study for some time. Chemical methods such as electropolishing (EP)[16, 17, 18], buffered chemical polishing (BCP)[17, 18], and oxy-polishing[17, 16] have been studied, but have failed to produce any meaningful improvement in surface roughness. The expected reason for this is that a large amount of material removal is required to produce a substantial smoothing effect when utilizing chemical methods. Electropolishing treatments for Nb typically remove between 5  $\mu\text{m}$  and 10  $\mu\text{m}$  of material to achieve a smooth surface depending on its initial roughness. This amount of material removal is infeasible for Nb<sub>3</sub>Sn films, since their thickness is only 2-3  $\mu\text{m}$ . Additionally, niobium and Sn react differently to the chemicals used, which can lead to different removal rates for each element, thus changing the surface stoichiometry. Even a small change in the stoichiometry away from Nb<sub>3</sub>Sn can cause a decrease in  $T_c$ [19].

To circumvent these issues, we instead use a technique known as centrifugal barrel polishing (CBP), a procedure commonly used for mechanically polishing Nb SRF cavities, and apply it to Nb<sub>3</sub>Sn cavities. First, Nb<sub>3</sub>Sn coated samples are polished to determine the effectiveness of the CBP method and to determine the optimum polishing parameters such as tumbling duration and the abrasive material. The results of the sample experiments are used to decide the polishing parameters for a Nb<sub>3</sub>Sn coated, 1.3 GHz, TESLA geometry SRF cavity. The RF performance of the cavity is tested before and after the CBP treatment. Finally, the cavity is treated with a low temperature Sn coating process to repair the surface and the RF performance is once again tested.

## 1.2 sample study

Since Nb<sub>3</sub>Sn is a relatively unexplored material, there are no established polishing parameters or abrasive materials to achieve a good surface finish. To allow for rapid iteration and microscopy surface analysis, we first perform polishing experiments on Nb<sub>3</sub>Sn samples. To evaluate the performance of CBP, the surface roughness of the polished samples is measured using confocal laser microscopy and the surface is analyzed using scanning and transmission electron microscopy (SEM and TEM). The material removal rate is measured using focused ion-beam tomography.

The samples were prepared using the standard Nb<sub>3</sub>Sn coating procedure. 1 cm disks are cut from a 4 mm sheet of fine-grain, low RRR niobium. 100  $\mu\text{m}$  of material are removed using standard electropolishing[20], followed by 5  $\mu\text{m}$  of removal using cold EP leading to a root-mean-square surface roughness of 20 nm for the initial substrate.[21] The samples are coated with the standard FNAL coating procedure.[7] This coating resulted in an approximately 3  $\mu\text{m}$  thick film with a grain size of 500 nm and a surface roughness of 200 nm as shown in Fig. 1.3. The grain size of the Nb substrate had no effect on the film grain size.

### 1.2.1 Centrifugal Barrel Polishing

Centrifugal barrel polishing (CBP) is another method used to polish SRF cavities utilizing an abrasive material to mechanically smooth the surface. Tumbling was first implemented for SRF cavities by KEK and Nomura Plating Co. in 1995[22]. This method has been used to repair surface damage and to attain a very smooth surface in Nb SRF cavities[23, 24].

As yet, only very limited attempts to apply this technique to Nb<sub>3</sub>Sn cavities have been made. The technique uses a custom-built tumbling machine that can fit up to 9-cell size 1.3 GHz cavities. When a cavity is mounted in the tumbling machine and filled with abrasive slurry, the rotating motion of the cavity accelerates the polishing media against the cavity surface at up to 59 m s<sup>-2</sup>.

The abrasive material determines the removal rate and minimum surface roughness attainable using CBP. Large-grit material is used to remove material quickly and smooth out large defects like pits and scratches while fine-grit material is used to microscopically smooth the surface. Since the roughness of as-coated Nb<sub>3</sub>Sn cavities is on the order of 100-200 nm, our experiments focus on using fine-grit materials. In this experiment, we use a colloidal nanoparticle suspension, purchased from Allied High Tech Products Incorporated, as our abrasive material. 50 nm diameter alumina and 40 nm diameter silica nanoparticles suspended in water were tested, but we found no discernible difference between the polishing characteristics of the two materials.

Silicon containing ceramics, such as silica, are a major concern for contamination in the tin coating furnace, since they can release a significant amount of silicon at high temperatures into the furnace. Silicon also reacts with Nb<sub>3</sub>Sn to form poorly superconducting silicide phases. Alumina, in contrast, is thermally stable at higher temperatures. This is why alumina is typically used to electrically insulate wires such as thermocouples inside the furnace. For these reasons, the alumina abrasive particles are preferable to avoid any risk of furnace contamination.

The nanoparticle suspension was mixed with a large, soft material to act as a carrier. The purpose of the carrier material is to carry the nanoparticles and to apply a force between them and the cavity surface. Two carrier materials were tested, 13 mm diameter wooden balls and 25 mm compressed wool cubes supplied by Congress Tools, Incorporated.

### 1.2.2 Coupon Cavity

To test the centrifugal barrel polishing method on Nb<sub>3</sub>Sn samples in a realistic environment, we use a coupon cavity[22]. This cavity has multiple ports where samples are mounted. The samples sit flush with the inside surface of the coupon cavity, as is shown in Fig. 1.1, where they experience identical polishing conditions to a real cavity surface. This allows for sample experiments that are representative of the final cavity polishing process. Using this method we inspect the Nb<sub>3</sub>Sn surface after polishing under a microscope to determine the best polishing parameters.

CBP was applied to samples mounted in the coupon cavity using the tumbling machine at FNAL. A total of four samples were polished for a duration of 2, 4, 6, and 8 h respectively. The machine was run at its maximum speed of 120 RPM for the entire duration.

### 1.2.3 Nb<sub>3</sub>Sn Coating Using Sn Vapor-Diffusion

The Nb<sub>3</sub>Sn samples used in this study were coated at Fermilab in a high-vacuum furnace. The coatings were created at 1,100 °C with a Sn crucible acting as the Sn source as well as SnCl<sub>2</sub> acting as a nucleating agent. A detailed review of the coating system at Fermilab shows the specific operating details of the coating system[7].

#### 1.2.4 Surface Analysis of Mechanically Polished Nb<sub>3</sub>Sn Coated Samples

The Nb<sub>3</sub>Sn samples were polished for different lengths of time ranging from 2 to 8 hours using the wooden spheres or the felt cubes as the carrier material. Height maps of the polished samples measured using confocal laser microscopy is shown in Fig. 1.2. The smoothness of the samples clearly improves as longer polishing is applied.

By comparing the surface optical micrographs after different amounts of polishing shown in Fig. 1.2, it is clear that material is preferentially removed from the highest point on the surface, causing the sharp peaks on the surface to be removed quickly while valleys are left untouched. The phenomenon is also clearly seen in SEM images of the samples shown in Fig. 1.5 where the peaks on the grains can be seen to become smoother and then flat as more polishing is applied. This is different from EP, which preferentially smooths areas with high curvature including both peaks and valleys. Due to this different smoothing mechanism, surface roughness is minimized when the thickness of material removed is equal to the height difference between the highest and lowest point on the surface, which is around 1  $\mu\text{m}$ . This is confirmed by the sample experiments, after 8 hours of polishing only the deepest valleys of the initial coating remain.

The surface height maps are used to calculate the root-mean-square (RMS) surface roughness of the samples and is shown in Fig. 1.3. After 6 hours of polishing the surface roughness is comparable to the surface roughness of the well performing, thinly coated Nb<sub>3</sub>Sn coatings created at FNAL[11]. We also calculate the power spectral density (PSD) of the surface profiles. The PSD is an indicator of the surface roughness at different length scales, indicated by the wavelength[25, 26].

This is verified by SEM micrographs of a thinly coated sample and a polished sample shown in Fig. 1.5A and D. After 8 hours of polishing, the surface roughness is comparable to a typical Nb surface after EP. This level of smoothness has never been achieved for Nb<sub>3</sub>Sn cavities until now. At this level of surface roughness, the performance degradation caused by field enhancement due to surface roughness should be greatly reduced.

The thickness of the film is measured after polishing using FIB/SEM cross-section measurements. Our measurements show that only a small amount of material is removed even after 8 hours of polishing. Fig. 1.4 shows the removal rate of different polishing materials. Samples polished using the felt media show an average removal rate of 170 nm/hour whereas the wooden media shows an average of 95 nm/hour removal rate. This measurement corresponds well with measurement performed on Nb cavities by Palczewski, Et. Al.[27] The starting thickness of the samples is between 3-3.5  $\mu\text{m}$ . After 8 hours of polishing there is still over 1.5  $\mu\text{m}$  of Nb<sub>3</sub>Sn left on the surface. To completely shield the Nb substrate from the RF fields only a few hundred nanometers of material are required, since the London penetration depth of Nb<sub>3</sub>Sn is approximately 100 nm[2].

The surface of the polished samples was analyzed using SEM and TEM to look for surface damage or chemical changes on the surface caused by the tumbling or cleaning process. As seen in Fig. 1.6 and Fig. 1.7, the Nb<sub>3</sub>Sn samples polished using wooden spheres were damaged resulting in microscopic scratches on the surface and a nanometer-scale damaged layer. The damaged layer is theorized to consist of disordered Nb<sub>3</sub>Sn layer as no atomic layers are visible and attempts to rotate the sample to align the zone axis in this region were unsuccessful. No surface damage was detected on samples polished using the felt cubes. The surface and oxide layer of the sample polished with felt cubes looks similar to the as coated surface[28, 29]. Since the surface damage may negatively

affect the cavity performance, the felt cubes are best to use for polishing Nb<sub>3</sub>Sn.

## 1.3 Polishing a Nb<sub>3</sub>Sn Cavity Using CBP

Given that CBP was able to produce a smooth surface on Nb<sub>3</sub>Sn samples, the next step is to apply the polishing to a Nb<sub>3</sub>Sn cavity. The cavity used as the substrate for this experiment is a 1.3 GHz niobium elliptical cavity. The cavity is made of 2.8 mm fine grain niobium with a residual resistivity ratio(RRR) of 300. However, this cavity was treated with nitrogen doping and electropolishing several times before being coated, which changes the actual thickness and RRR. In preparation for the coating, the cavity was electropolished for 100  $\mu\text{m}$  using standard EP and an additional 5  $\mu\text{m}$  of cold EP to achieve a smooth surface. Before the coating the cavity was anodized to improve the nucleation of Nb<sub>3</sub>Sn grains. During the coating, the cavity was heated to the nucleation temperature at a rate of 3  $^{\circ}\text{C min}^{-1}$  to 500  $^{\circ}\text{C}$  and held for 5 hours. The temperature was then increased to 1100  $^{\circ}\text{C}$  at a rate of 3  $^{\circ}\text{C min}^{-1}$  and held for another 5 hours. The Sn source heater was set to 713  $^{\circ}\text{C}$  for the nucleation stage and 1325  $^{\circ}\text{C}$  for the coating stage.

The Nb<sub>3</sub>Sn-coated cavity was polished using the felt cube polishing media with a 50 nm alumina abrasive particle suspension. The cavity was polished for 4 hours at 120 RPM using the tumbling machine described in section 1.2.1 followed by high-pressure water rinsing and ultrasonic cleaning for 30 minutes to remove any residual abrasive material left by the polishing process. The polishing duration was chosen as a conservative estimate to minimize the possibility of removing the Nb<sub>3</sub>Sn film during polishing and allow for more material removal in the future while still providing a considerable improvement in surface roughness.

Visual inspection of the cavity shows that the surface roughness was improved by the polishing procedure. The as-coated surface of the cavity has a matte finish, which is common on Nb<sub>3</sub>Sn-coated surfaces, and after the polishing the cavity has a shiny surface finish. This is indicative of the removal of microscopic surface roughness on the surface of the cavity.

### 1.3.1 Low Temperature Recoating Procedure

After the Nb<sub>3</sub>Sn-coated cavity was polished using CBP, a secondary coating was applied, which we refer to as the recoating procedure. The purpose of this coating is to repair any surface damage caused by CBP or any subsurface defects, such as tin-deficient regions, that may have been exposed.

For the recoating procedure, the furnace temperature was ramped up to 1,000  $^{\circ}\text{C}$  at a rate of 3  $^{\circ}\text{C min}^{-1}$  and then held for one hour. At the same time the Sn source heater temperature was ramped to and held at 1300  $^{\circ}\text{C}$ . This lower temperature was chosen to minimize any thermal etching of the surface, which could increase the surface roughness. No SnCl<sub>2</sub> was used as it is unnecessary to nucleate any Nb<sub>3</sub>Sn grains. One third of the normal amount of Sn, 0.85 g, was used during the coating. The coating was performed at Fermilab using the coating furnace mentioned in Section 1.2.3.

### 1.3.2 SRF Cavity RF-Performance Testing

The RF performance of the Nb<sub>3</sub>Sn-coated cavity was tested three times; first, in the as-coated state with no polishing applied; second, after the CBP treatment; lastly, after the recoating procedure. The performance was tested using the vertical test stand (VTS) at FNAL[30].

### 1.3.3 Testing the Polished Nb<sub>3</sub>Sn SRF Cavity

The as-coated performance of the cavity was poor compared to most other Nb<sub>3</sub>Sn cavities reaching an accelerating gradient of around 10 MV/m with a Q of 10<sup>10</sup> at 4.4 K. The quality factor exhibits an unusual decrease around 6 MV/m at 2.0 K which does not appear at 4.4 K. The cause of this decrease is unknown, but may be due to a surface defect with a lower T<sub>c</sub> such as a tin-depleted regions which becomes normal conducting as the accelerating gradient increases.

After the polishing is applied, the cavity exhibits Q-slope (the quality factor decreases with increasing accelerating field), and the maximum gradient was only 5 MV/m. The cavity was then treated with the recoating treatment, detailed in Section 1.3.1, the Q-slope is ameliorated and the maximum accelerating gradient increases to 15 MV/m. The quality factor dip seen in the as-coated state at 2.0 K was also removed, which could indicate the removal of a surface defect, but the quality factor at 4.4 K remained unchanged. Fig. 1.8 shows the performance of the cavity after each step.

## 1.4 Discussion

Using mechanical polishing, we are able to produce smooth Nb<sub>3</sub>Sn films with surface roughness less than 20 nm. This level of surface roughness has thus far been impossible to achieve using existing methods.[11, 16, 17, 18] We have also shown that this smoothing can be achieved with only a few hundred nanometers of material removal, much less than what would be required for chemical polishing methods.

This study also shows that mechanical polishing can be used to improve the performance of Nb<sub>3</sub>Sn cavities when used in conjunction with a recoating procedure. There are several reasons why polishing a Nb<sub>3</sub>Sn might lead to performance improvements. The most obvious is the reduction in surface roughness, which reduces the field enhancement factor around sharp edges. This should lead to a decrease in Q-slope and an increase in quench field[12, 13] due to a reduction in the volume of normal conducting material interacting with the RF field. However, only one of these effects is experimentally measured, the increase in quench field, while the Q-slope remains mostly unchanged.

Another effect of polishing is a reduction in the film thickness. Nb<sub>3</sub>Sn is a poor thermal conductor compared to Nb, which can lead to a buildup of heat on the cavity surface. Higher surface temperatures lower the super heating critical magnetic field and increases BCS resistance causing a premature quench. By decreasing the film thickness, the thermal properties are improved which could lead to a higher quench field[31]. From our sample experiments we measured a removal of approximately 700 nm after 4 hours of polishing. Assuming a 3 μm starting thickness and one dimensional heat diffusion through the film, this reduction could lead to a 30% increase in the maximum heat flux. This effect is more significant if there is a point source of heat on the surface caused by a defect[32]. In this case, the quench field is determined by the thermal stability of the

defect. A reduction in film thickness can lead to better thermal stability and allow the cavity to reach higher gradients.

The immediate effect of polishing reduces the quality factor and accelerating gradient of the cavity despite improving the surface finish and decreasing film thickness. The exact cause of this performance degradation is not known. There are two types of defects that could cause a degradation in performance; pre-existing subsurface defects that were created during the initial coating of the cavity and defects that were created by the tumbling process.

Pre-existing defects existing below the surface of the as coated film such as tin-depleted regions[33] and other poorly conducting Nb<sub>3</sub>Sn phases are known to exist below the surface of the film and could be exposed to the surface by the removal of material through polishing. In a previous study, we have shown that tin-depleted regions and regions where the film becomes very thin are common in tin vapor-diffusion coated samples near the surface were they could be exposed by the polishing process[34].

Another possible cause for performance degradation is surface damage or other defects caused by the polishing process. Residual abrasive particles can be seen in the SEM images of the polished samples. Cleaning the surface removes most of the contamination, but there may still be some abrasive particles left on the surface, which could cause performance degradation. Surface damage such as cracks or scratches on the film could also degrade performance, although this seems unlikely as no surface damage was detected on the Nb<sub>3</sub>Sn samples polished with felt cubes. It is also possible that the oxide that forms on the Nb<sub>3</sub>Sn surface after polishing is unfavorable for performance compared to the oxide that forms in the furnace after the coating process.

After the recoating process was applied, the cavity performance was improved over the unpolished state. We theorize that the re-coating procedure can eliminate both of the aforementioned defect types. A short, low-temperature coating is sufficient to diffuse more Sn into any exposed tin-depleted regions that may have been exposed during the polishing. It is also possible that the Sn vapor can diffuse into and repair any small cracks that may have been created during tumbling. Also, by raising the temperature of the Nb<sub>3</sub>Sn, the surface oxide layer created during the tumbling is dissolved, and a new surface oxide is created when the cavity is exposed to air. Only the residual alumina particles are unaffected by the recoating, since they are thermally stable at 1000 °C. However, it is difficult to determine the exact effects of the recoating without performing a thorough cutout analysis on the cavity. Further studies are under way to determine the cause of the performance degradation after mechanical polishing and the effects of the recoating procedure on the Nb<sub>3</sub>Sn surface.

It is also worth studying the recoating process on its own to determine if there is any effect on unpolished cavities. The extra Sn provided by the recoating could improve the stoichiometry of the surface and eliminate tin-deficient regions. Additionally, the effects of annealing the cavity at 1000 °C could also be causing a performance increase.

Even after polishing and recoating, the accelerating gradient of the mechanically polished cavity is still below that of the current record holding cavity[11]. This suggests that there are multiple mechanisms that contribute towards cavity quench with surface roughness being one of them. By using mechanical polishing to eliminate the effects of surface roughness on the cavity performance, we can isolate these other mechanisms. We plan to apply mechanical polishing to Nb<sub>3</sub>Sn cavities with better as-coated performance. If the performance improvement shown in this paper can be realized in cavities with better initial performance, we could see a drastic increase in the maximum accelerating

gradient.

Utilizing CBP for Nb<sub>3</sub>Sn SRF cavities is still an under-explored process, and the research presented in this paper only shows our initial attempts at optimizing the process. At the moment we have only a single cavity to base our results on, which limits our ability to understand the process. There are many parameters that can be tweaked to potentially improve the cavity performance, and many questions that are left unanswered. Therefore, we must polish more cavities to understand the effects of each step of the process on the final performance.

We still do not know the effect residual abrasive particles have on the cavity performance. The alumina abrasive is not expected to contribute any significant resistive losses, but could contribute dielectric losses. The combination of ultrasonic cleaning and HPR shown in this study is likely not sufficient to entirely remove residual abrasives. Further research is necessary to find a reliable cleaning method for polished cavities. Chemical cleaning methods such as HF rinsing may be promising in this regard. Further polishing could help prevent alumina from sticking to the surface by removing crevices that alumina can gather in.

Another step that must be studied further is the recoating. The temperature, duration, and amount of Sn used are chosen to minimize any surface roughness caused by the recoating due to thermal etching mechanisms and also to prevent the growth of an excessively thick film which could negatively impact the thermal characteristics of the cavity. However, it is unclear how prominent thermal etching is or what other impact these parameters have on the film microstructure. Work still needs to be done to determine the optimum parameters for repairing the damage caused by the polishing while also minimizing any thermal etching and negative side effects. It is also worth investigating the effects of the recoating on unpolished cavities to see if any performance improvements can be made by introducing more Sn at a lower temperature after the initial coating is complete.

The ability to smooth the surface of the Nb<sub>3</sub>Sn cavities also opens opportunities to experiment with coatings of different thicknesses and grain structure which can then be polished to achieve a smoother surface than is currently possible. Having precise control of the coating thickness as well as the removal rate of the polishing step could allow for much thinner and smoother films with better thermal conduction properties. Future research should incorporate Nb<sub>3</sub>Sn coatings with different initial thicknesses.

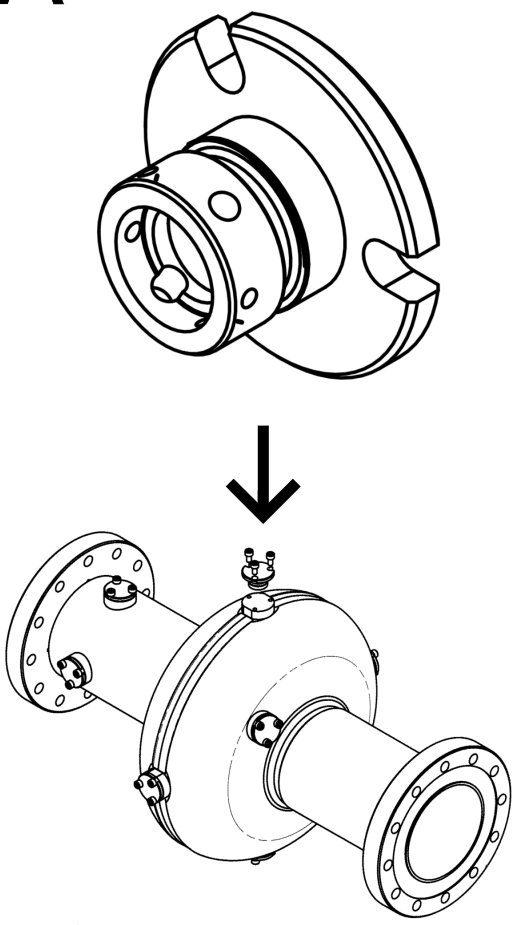
## 1.5 Conclusion

The work presented in this paper shows that centrifugal barrel polishing is a promising treatment for Nb<sub>3</sub>Sn cavities. Through a series of sample studies, we were able to develop a mechanical polishing procedure that can produce surface roughness that was previously unobtainable. We have found that it is possible to attain films with a surface roughness of 20 nm or lower.

Furthermore, we have shown that this surface polishing technique can be used to improve the performance of Nb<sub>3</sub>Sn coated cavities when it is paired with a recoating step, which consists of a short, low-temperature Sn coating.

We also stress the fact that centrifugal barrel polishing is still a highly unexplored process for Nb<sub>3</sub>Sn SRF cavities. More research is needed to find the optimum parameters for improving cavity performance.

A



B

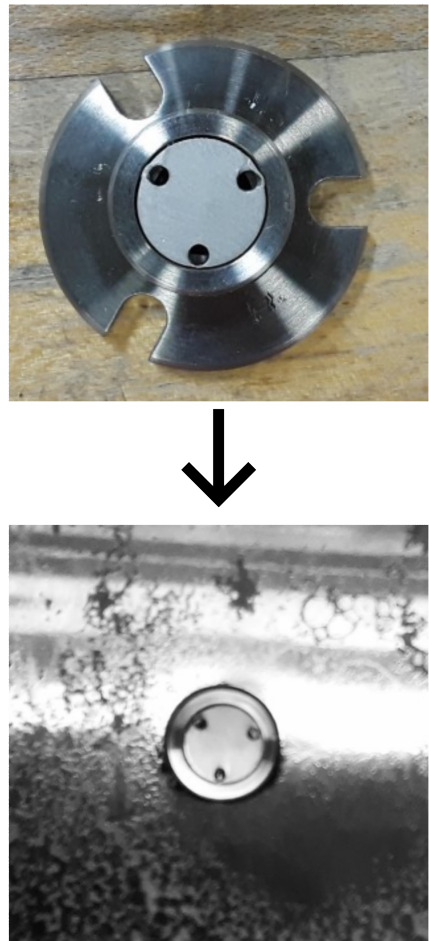
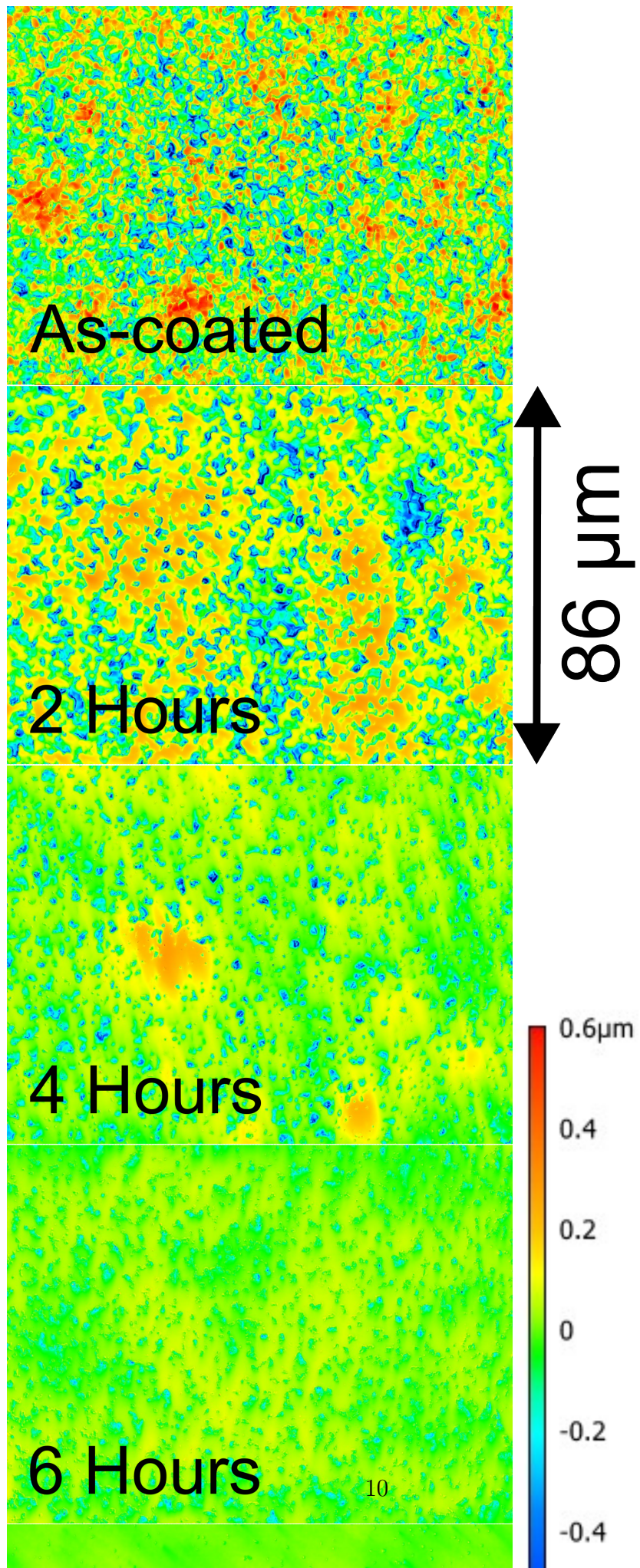


Figure 1.1: (A) A schematic of the coupon cavity and the sample holder used to polish the Nb<sub>3</sub>Sn coated samples. The sample holder can hold 1 cm diameter disks by clamping the sides of the sample with set screws. (B) Pictures of the sample holder sitting outside the coupon cavity with a sample mounted and as seen from the inside of the coupon cavity.



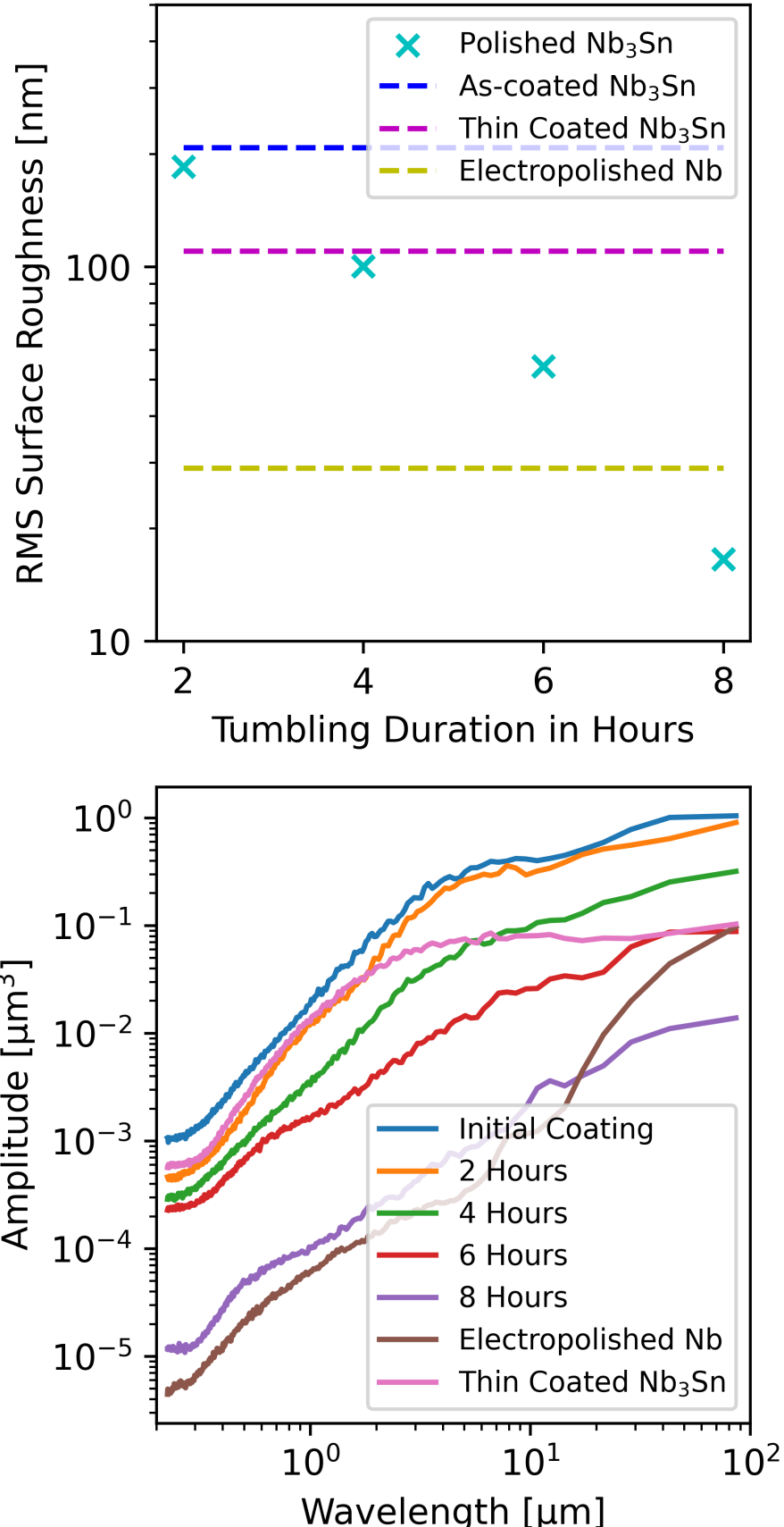


Figure 1.3: Surface roughness of Nb<sub>3</sub>Sn samples mechanically polished for different lengths of time calculated from the surface height maps (top). The power spectral density (PSD) of the surface profile after different amounts of tumbling as well as the PSD of electropolished Nb and a thinly coated Nb<sub>3</sub>Sn[11] film (bottom). The PSD is an indicator of the surface roughness of the sample at different length scales.

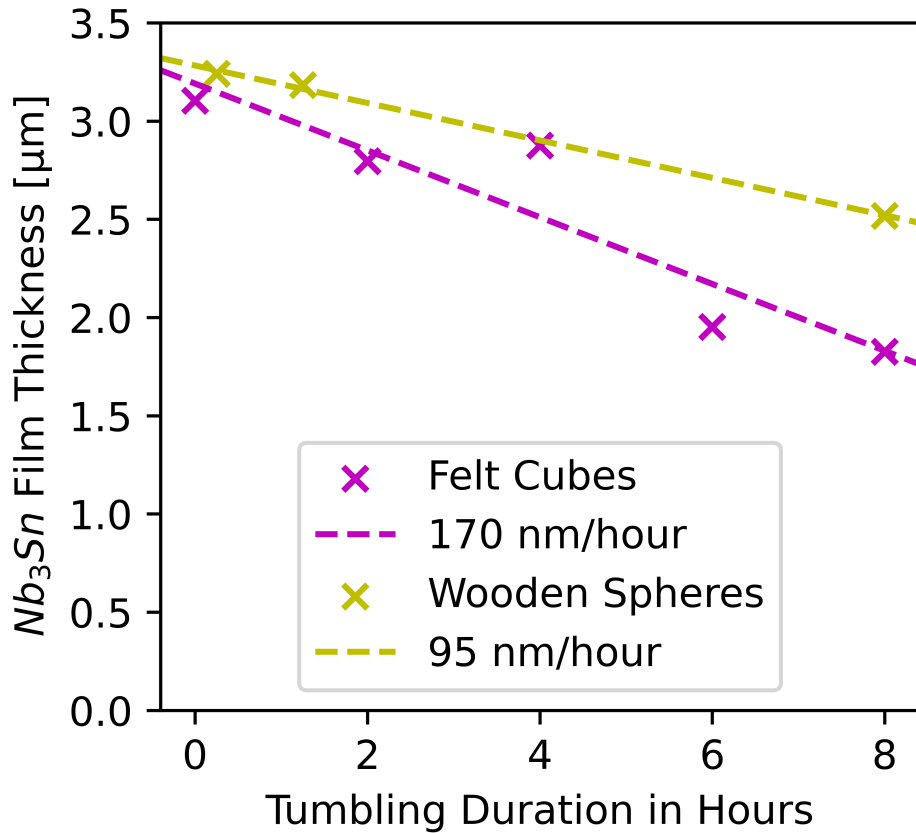


Figure 1.4: The thickness of the  $\text{Nb}_3\text{Sn}$  film after mechanically polished for different lengths of time using felt cubes or wooden spheres as the polishing media.

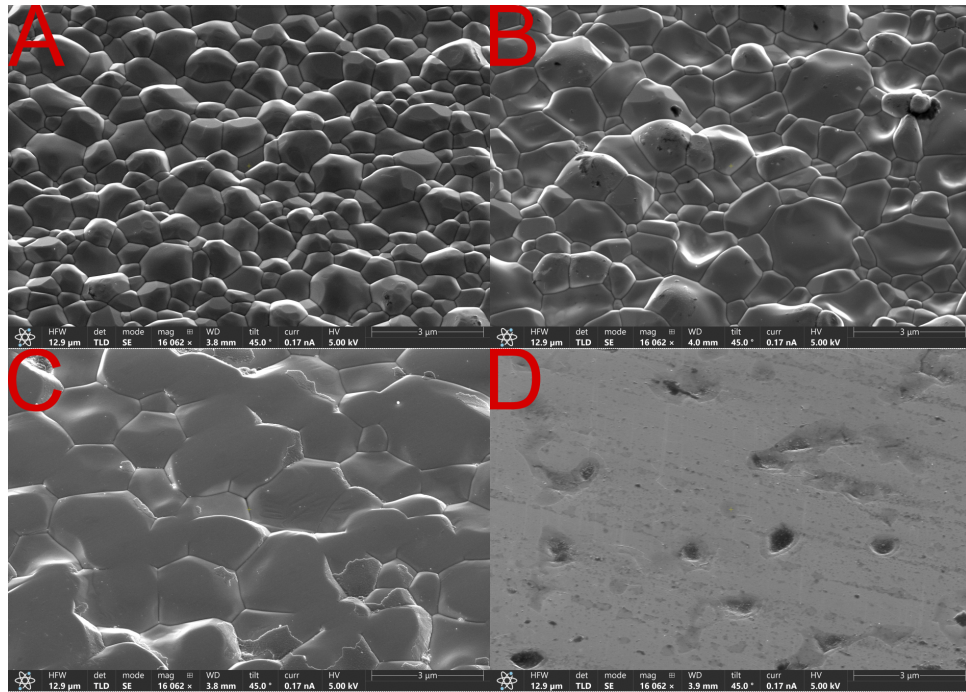


Figure 1.5: SEM micrographs of a  $\text{Nb}_3\text{Sn}$  a thin coated sample (A), standard coated sample (B), a sample after polishing for 2 hours (C), and a sample after polishing for 6 hours (D).

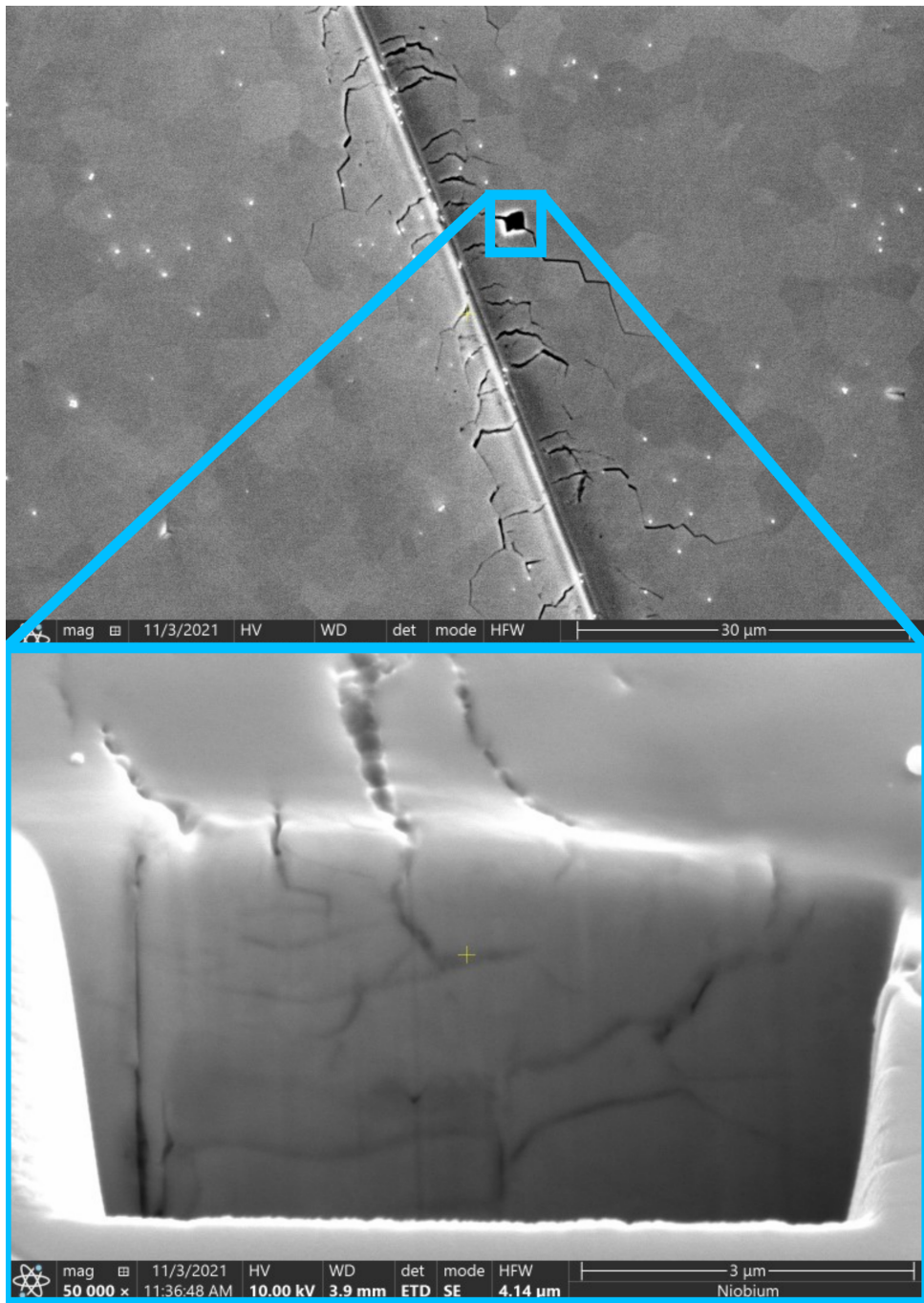


Figure 1.6: SEM micrograph showing a Nb<sub>3</sub>Sn sample polished for 30 hours using wooden spheres and a colloidal abrasive suspension. Nb<sub>3</sub>Sn films polished using wooden spheres show microscopic scratches and cracks on the surface. A square hole is cut into the surface, visible in the top micrograph to expose a cross-section of a crack. The cross-section shows that the cracks penetrate deep into the film.

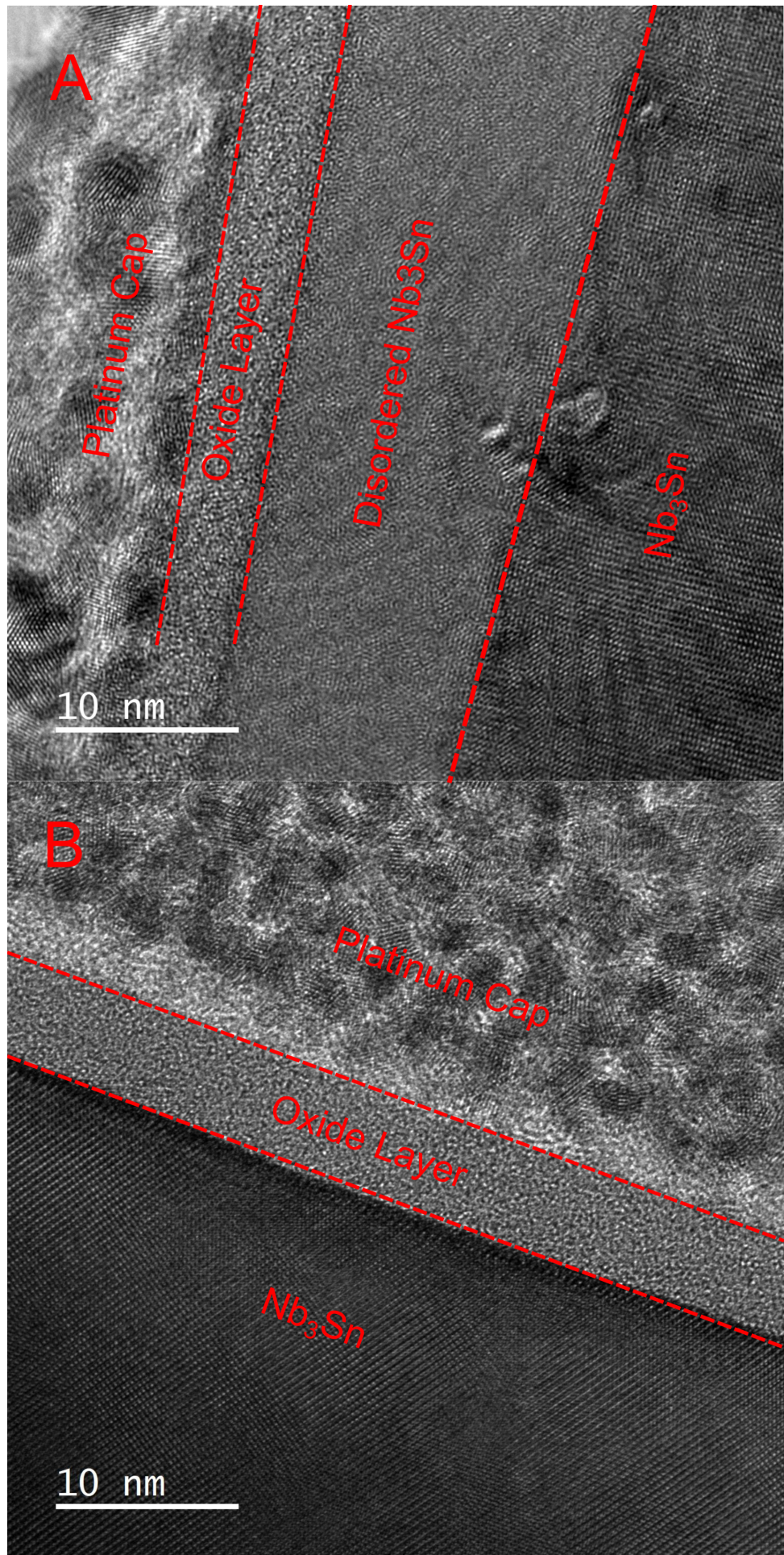
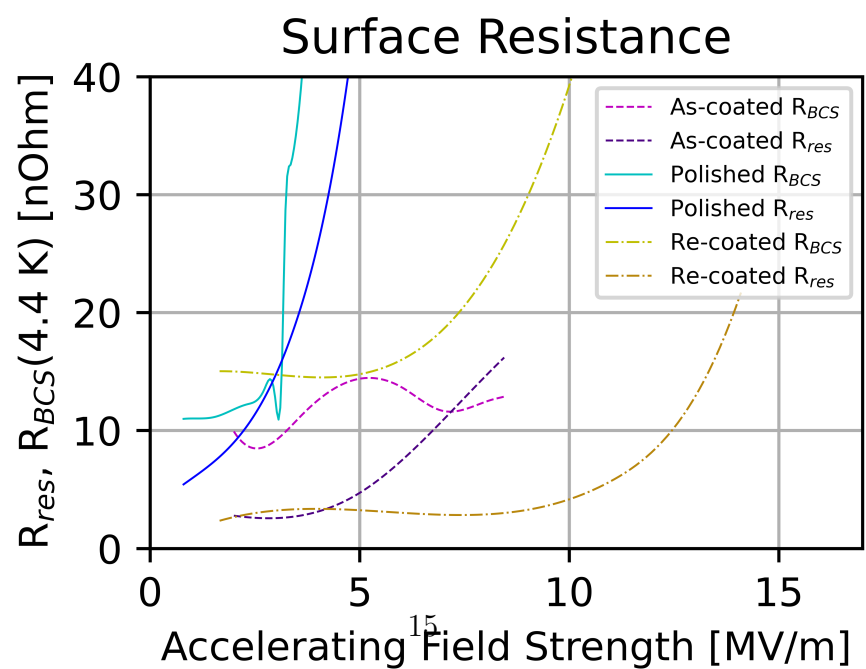
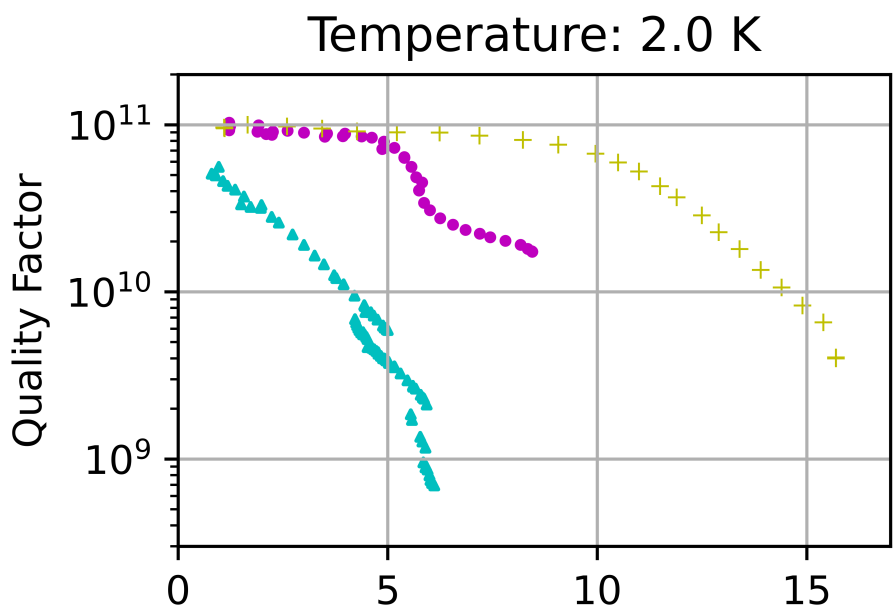
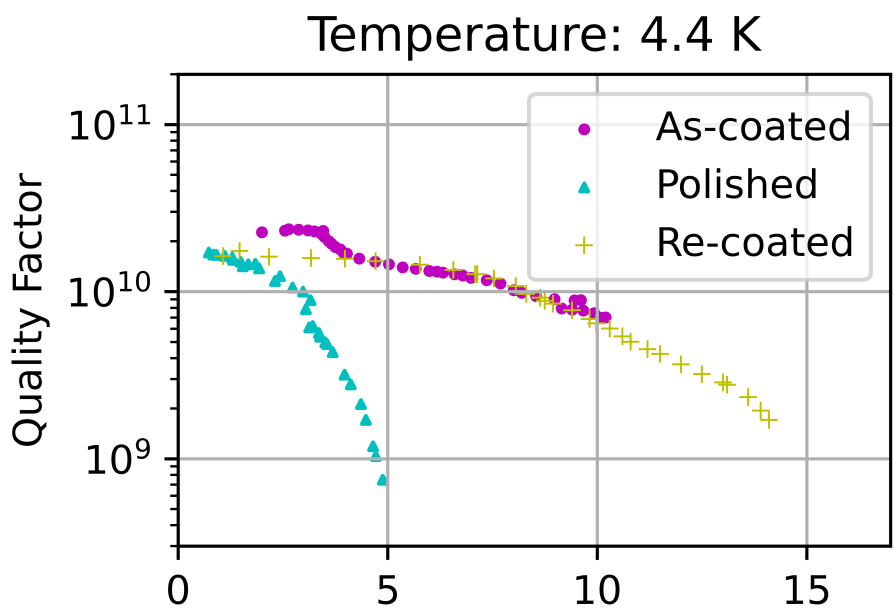


Figure 1.7: TEM images of a  $Nb_3Sn$  sample polished using wooden spheres (A) and felt cubes (B). The polishing procedure creates a 10 nm thick layer of disordered  $Nb_3Sn$ , shown to be below the layer of oxide at the top and the layer of disordered  $Nb_3Sn$ .



# Chapter 2

## Recoating

### 2.1 Introduction

Niobium cavities have been extensively studied and treatments have been developed to optimize the accelerating gradient and quality factor [?, ?, ?, ?]. The performance of niobium SRF cavities is limited by the material properties of niobium (Nb). A promising alternative to Nb is Nb<sub>3</sub>Sn. There exists a large body of research on creating high performance Nb<sub>3</sub>Sn superconducting radiofrequency (SRF) cavities[?, ?]. Desirable superconducting properties, such as higher superconducting transition temperature (T<sub>c</sub>) and a higher superheating magnetic field (H<sub>sh</sub>)[2, 3, 4, 5], make Nb<sub>3</sub>Sn an attractive material for SRF applications. The material properties of Nb<sub>3</sub>Sn, however, make it difficult to work with.

The brittleness of Nb<sub>3</sub>Sn introduces new challenges to the cavity manufacturing process. Nb<sub>3</sub>Sn must be deposited as a thin film on a bulk cavity substrate[7, 8, 9]. Because of the thin and brittle film, Nb<sub>3</sub>Sn cavities are highly susceptible to mechanical stress. Nb<sub>3</sub>Sn cavity performance is known to permanently degrade when stresses are applied to the cavity[?, ?]. This degradation is assumed to be caused by cracks in the brittle Nb<sub>3</sub>Sn film caused by deformation of a cavity during processing such as tuning or assembly. Cavities that suffer from degradation are typically stripped and recoated with a new Nb<sub>3</sub>Sn film, which is a time-consuming and expensive process.

In this current study we explore a new procedure to heal Nb<sub>3</sub>Sn cavities whose performance has been degraded by deformation. This procedure utilizes a short Nb<sub>3</sub>Sn recoating to attempt to heal cracks that have formed in the cavity without the need to remove the original film. This procedure was developed to restore the performance of a Nb<sub>3</sub>Sn cavity which has undergone centrifugal barrel polishing[?]. The performance decrease measured on a polished cavity is like the above mentioned case of deformation-induced degradation. When employing this recoating procedure to a degraded cavity, we can recover a large portion of the performance with a simple furnace treatment. This discovery provides a valuable method for recovering degraded cavities without lengthy reprocessing which avoid subsequent thinning and frequency shifts.

### 2.2 Experiment

This study is performed on a Nb<sub>3</sub>Sn, 1.3 GHz cavity coated using a high-temperature nucleation step to create a Nb<sub>3</sub>Sn film with low surface roughness. An in-depth analysis of

this cavity coating and the initial performance of the cavity can be found in reference [11].

After initial testing, the cavity was transported to Cornell, after which performance decreased. The cavity was then returned back to FNAL for additional testing, which confirmed the performance degradation. We suggest that the degradation was caused by stresses applied to the cavity during transport, which led to the formation of cracks. This type of performance degradation has previously been observed during assembly of Nb<sub>3</sub>Sn cavities [?], and when tuning Nb<sub>3</sub>Sn cavities at room temperature [?]. In these cases, stresses applied to the cavity were suggested to be the main cause of the degradation. Cracks may also form in Nb<sub>3</sub>Sn cavities as a result of stress concentrators such as foreign particles or impurities located in the Nb-Nb<sub>3</sub>Sn interface. Another possible source of performance degradation is elastic deformation of the Nb<sub>3</sub>Sn film caused by thermal contraction of the cavity during cooldown. This is, however, unlikely in this case since the thermal expansion coefficient of Nb and Nb<sub>3</sub>Sn does not differ enough to cause degradation, and Nb<sub>3</sub>Sn cavities have shown no signs of degradation due to thermal cycling.

To heal the cracks causing the performance degradation, we apply a recoating procedure. During this recoating procedure, the cavity was heated to 1000 °C and exposed to Sn vapor for 1 h. Sn vapor was provided by 0.85 g of Sn heated to 1250 °C. The reasoning behind these parameters is that only a small amount of Sn is necessary to fill the microscopic cracks in the film. Applying too much Sn causes the film to become too thick and negatively impacts the surface roughness of the film. During the coating process only a small fraction of the Sn evaporated leaving behind a large amount of the initial Sn still in the crucible.

The cavity performance was tested using a vertical testing stand (VTS). The cavity was tested before degradation, after degradation, and after recoating at 4 K and at 2 K. The cavity was cooled down below its superconducting transition temperature at 16 K at a slow cooling rate of 0.1 K min<sup>-1</sup> to minimize trapped flux. Between each test the cavity was brought up to a temperature above its superconducting transition temperature and cooled back down using the slow cooling rate to eliminate any trapped flux caused by cavity quenching. Temperature mapping was performed during the VTS test at 2 K.

## 2.3 Results

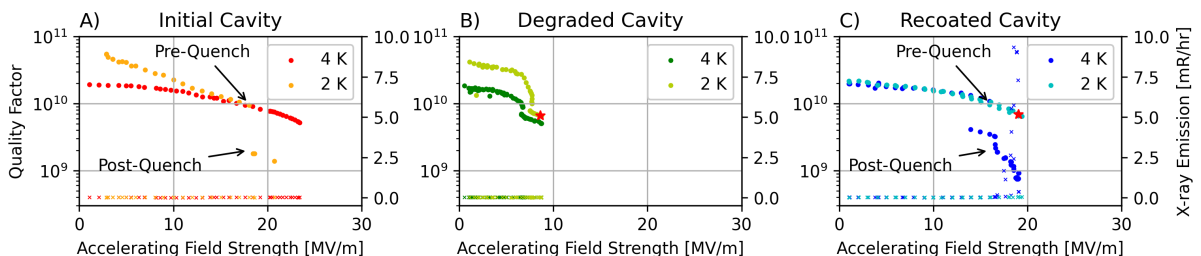


Figure 2.1: The quality factor, indicated by dots, and X-ray emissions, indicated by x, versus the accelerating gradient of the cavity after the initial coating (A), after the degradation (B), and after the recoating (C). The quality factor and accelerating gradient of the T-maps in figure 2.2 are indicated by a red star.

After initially coating the cavity it achieves a peak accelerating field of  $24 \text{ MV m}^{-1}$  and a maximum Q of  $2 \times 10^{10}$  at 4 K. The peak accelerating gradient after degradation is  $8 \text{ MV m}^{-1}$  and a maximum Q of  $2 \times 10^{10}$  at 4 K. The cavity displays a decrease in the quality factor at around  $6 \text{ MV m}^{-1}$  before a quench. A similar decrease in the quality factor is observed for other cavities affected by performance degradation[?, ?] and in Nb<sub>3</sub>Sn cavities treated with centrifugal barrel polishing[?]. Temperature mapping is displayed in figure 2.2 and is utilized to locate the quench source responsible for the performance degradation. A single hot spot on the equator of the cavity is present. Visual inspection of the cavity did not display visible defects near the quench location.

After the recoating procedure is applied the cavity's performance increases. The cavity experiences an initial quench at  $16 \text{ MV m}^{-1}$  resulting in trapped flux which decreases the quality factor. The cavity is still able to reach a peak accelerating gradient of  $19 \text{ MV m}^{-1}$ . At 2 K the cavity does not quench until reaching the maximum gradient of  $19 \text{ MV m}^{-1}$ . The quality factor after recoating is  $2 \times 10^{10}$  at 4 K and the Q slope seen in the degraded cavity is not present. Temperature mapping of the cavity after recoating demonstrates that the initial hot spot is healed with no detectable heating from that area. This indicates that the defect causing the performance degradation is repaired by recoating. At higher gradients another small hotspot appears in a new location close to the equator, and there is also a larger hot spot closer to the iris, which appears just before the cavity quench. We also see a spike in the x-ray emissions from the cavity just before the final quench at 4 K. Although we are not certain what the cause of this spike is, it does not seem to be caused by the cracks nor the recoating. This particular cavity has shown x-ray emissions in the past even before the degradation and recoating occurred.

## 2.4 Evidence of Crack Healing Mechanism in Nb<sub>3</sub>Sn

To study the healing mechanism of the recoating procedure, we purposefully introduce cracks into Nb<sub>3</sub>Sn coated Nb wires. 3 mm diameter low RRR Nb wires were coated with Nb<sub>3</sub>Sn using Sn vapor diffusion. Before the coating, the Nb wires are electropolished and anodized in the same way as Nb<sub>3</sub>Sn cavities. Cracks are created by elongating the wires using an Instron tensile testing machine. We then cut the wires into two pieces and treat one half of the wires with the same recoating recipe shown in section 2.2. The cracks are analyzed before and after recoating using scanning electron microscopy (SEM) and energy dispersive x-ray spectroscopy (EDS).

The elongation of the wires causes intragranular cracks to form perpendicular to the direction of applied stress as shown in figure 2.3. A cross section of the sample, as seen in figure 2.4, show that the cracks penetrate all the way through the Nb<sub>3</sub>Sn film and stop at the Nb substrate giving the crack a rectangular profile with sharp 90° edges. These cracks can be considered an extreme example of the cracks we expect to see in Nb<sub>3</sub>Sn cavities since the wires are heavily deformed in the plastic regime. In contrast, cracks formed in Nb<sub>3</sub>Sn cavities are formed during elastic deformation of the niobium substrate or only slight plastic deformation which does not significantly impact the geometry of the cavity. Therefore, we expect cracks in degraded cavities to be smaller than what is seen in this study.

After the recoating, the cracks appear to be partially healed. Figure 2.3 shows some of the cracks being partially filled in with new material creating a discontinuous crack. Additionally, the sharp edges of the untreated cracks have been smoothed out due to

deposition of new material. The cross section of the sample in figure 2.4 shows that new Nb<sub>3</sub>Sn is created both within the crack and at the exposed Nb substrate at the base of the crack. Since the cracks produced by elongating the wires are larger than what we expect in Nb<sub>3</sub>Sn cavities, it is likely that the cracks formed in cavities can be completely healed using this recoating recipe. It may also be possible to increase the recoating duration or temperature to allow larger cracks to heal completely as well.

## Discussion

Recoating a damaged Nb<sub>3</sub>Sn cavity can have a major impact on its performance. The recoating process was able to mostly recover both the maximum accelerating gradient and quality factor of the cavity. The degradation in quality factor seen at 2 K at high fields seen in figure 2.1, C is caused by a quench at 16 MV m<sup>-1</sup> resulting in trapped flux. However, the cavity was able to reach a higher gradient of 19 MV m<sup>-1</sup> after the initial quench. This is close to the 24 MV m<sup>-1</sup> maximum field of the cavity before the degradation occurred. It is possible that the cavity may recover more of its performance by using a longer recoating or other surface treatments such as mechanical polishing[?].

The healing mechanism of the recoating is heretofore unknown. From our observations it appears that the healing occurs via two different processes, the creation of new Nb<sub>3</sub>Sn within the crack and the creation of Nb<sub>3</sub>Sn at the exposed Nb substrate at the base of the crack. This phenomenon has been studied in other thin film system and is known as self healing [?]. Here we propose two mechanisms to explain the self healing observed in our experiments.

The first mechanism for self healing is creation of newly formed Nb<sub>3</sub>Sn within the crack. When a cavity is exposed to Sn, a thin layer of liquid Sn coats the surface which thereby fills the cracks. Nb<sub>3</sub>Sn is then formed in the cracks by diffusion of Nb from the old Nb<sub>3</sub>Sn into the liquid Sn creating new Nb<sub>3</sub>Sn. The diffusion rate of Nb is relatively slow compared to the diffusion of Sn through the grain boundaries during normal film growth, however if the cracks are small, less than a few 100 nm, Nb may have sufficient time to diffuse into the crack. The diffusion of Nb into the crack may be aided by dissolution of Nb<sub>3</sub>Sn into the liquid Sn layer above 910 °C which would greatly boost the diffusion rate. Since Nb is diffusing from the Nb<sub>3</sub>Sn film into the crack, there is the possibility of creating non-superconducting Sn rich Nb-Sn phases such as Nb<sub>6</sub>Sn<sub>5</sub> and NbSn<sub>2</sub>. However, we see no evidence of these phases on the length scales measurable using EDS. Further analysis is required using higher resolution techniques such as transmission electron microscopy (TEM-EDS) to verify the stoichiometry of the newly created Nb<sub>3</sub>Sn material.

The second mechanism involves the diffusion of Sn into the Nb substrate through the crack. Since the crack penetrates the Nb<sub>3</sub>Sn film, the liquid Sn layer can come into contact with the crack and react with the Nb substrate creating a region of new Nb<sub>3</sub>Sn. This new region acts as a bridge for electrical currents to flow through the film and prevents current from flowing through the Nb substrate, which has a higher resistivity than does Nb<sub>3</sub>Sn.

## 2.5 Conclusion

Using a low temperature (1000 °C), short duration (1 h) Sn recoating process, we are able to heal a degraded Nb<sub>3</sub>Sn cavity that suffered damage during transportation. The recoat-

ing process improved the maximum gradient of the cavity from  $8 \text{ MV m}^{-1}$  to  $19 \text{ MV m}^{-1}$ , which is close to the initial performance of the cavity of  $24 \text{ MV m}^{-1}$ . Temperature mapping measurements of the cavity demonstrate that a single hot spot on the equator of the cavity was responsible for the performance degradation. After the recoating process this defect becomes healed leading to less heating and a higher maximum electric field gradient. Ultimately, the performance is limited by a second hot spot.

This discovery provides a new approach which applies to similarly degraded SRF cavities to recover their performances. This approach saves time and money which would otherwise be spent removing the Nb<sub>3</sub>Sn coating and then applying a new coating. This self healing process makes Nb<sub>3</sub>Sn cavities more viable for real-world accelerator applications by reducing their manufacturing costs.

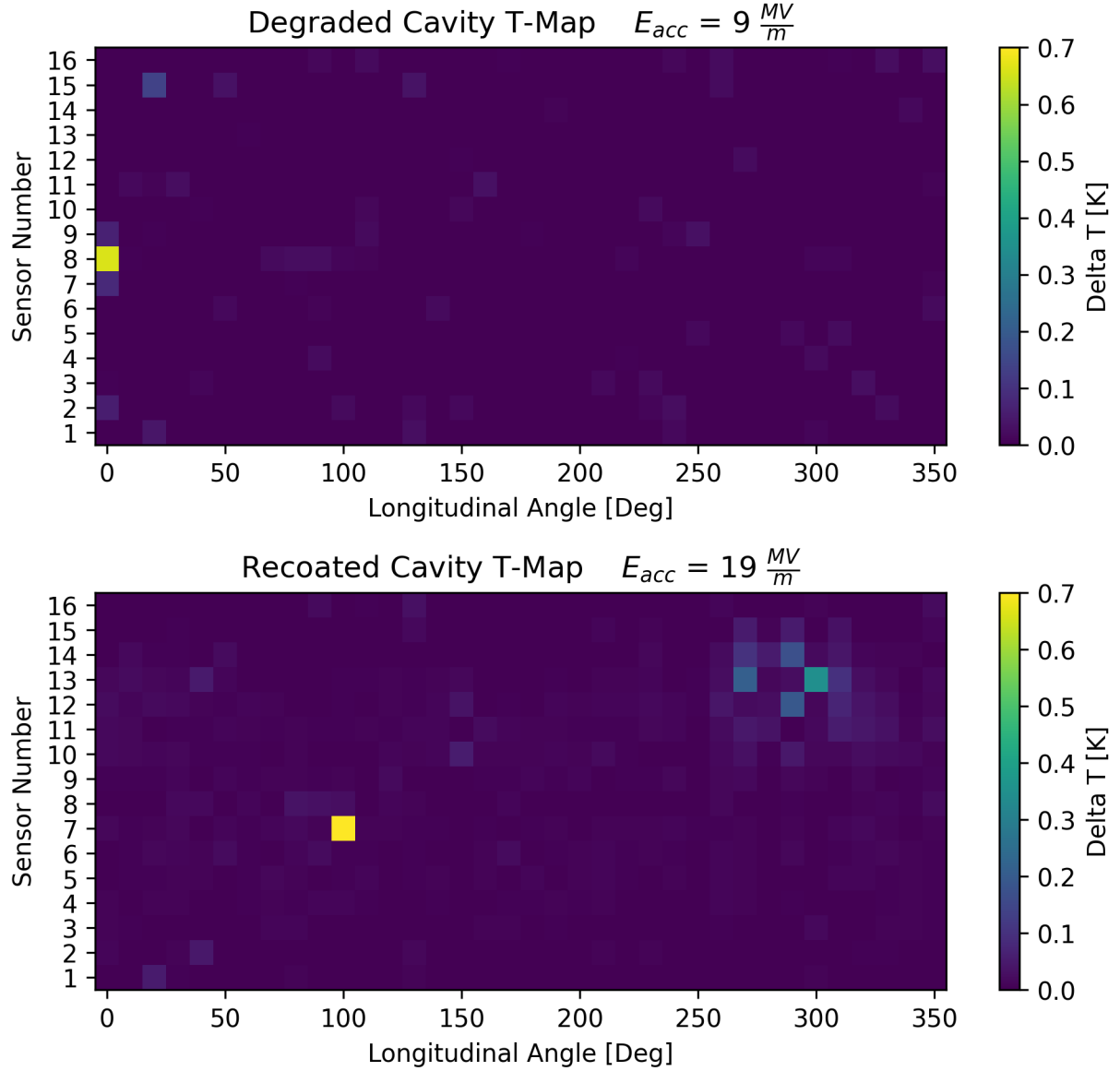


Figure 2.2: Temperature maps of a cavity's surface prior to quench as measured before (top) and after (bottom) the recoating is applied. The temperature maps are measured at 2 K. The sensor number corresponds to different regions of the cavity. Sensor 1 and 16 are near the top and bottom iris while sensor 8 is on the equator. The quality factor and accelerating gradient of the cavity during the measurement is shown by the red star in figure 2.1. The temperature of the hot spot near the equator of the recoated cavity exceeds the maximum value of the color bar and achieves a maximum value at 3 K

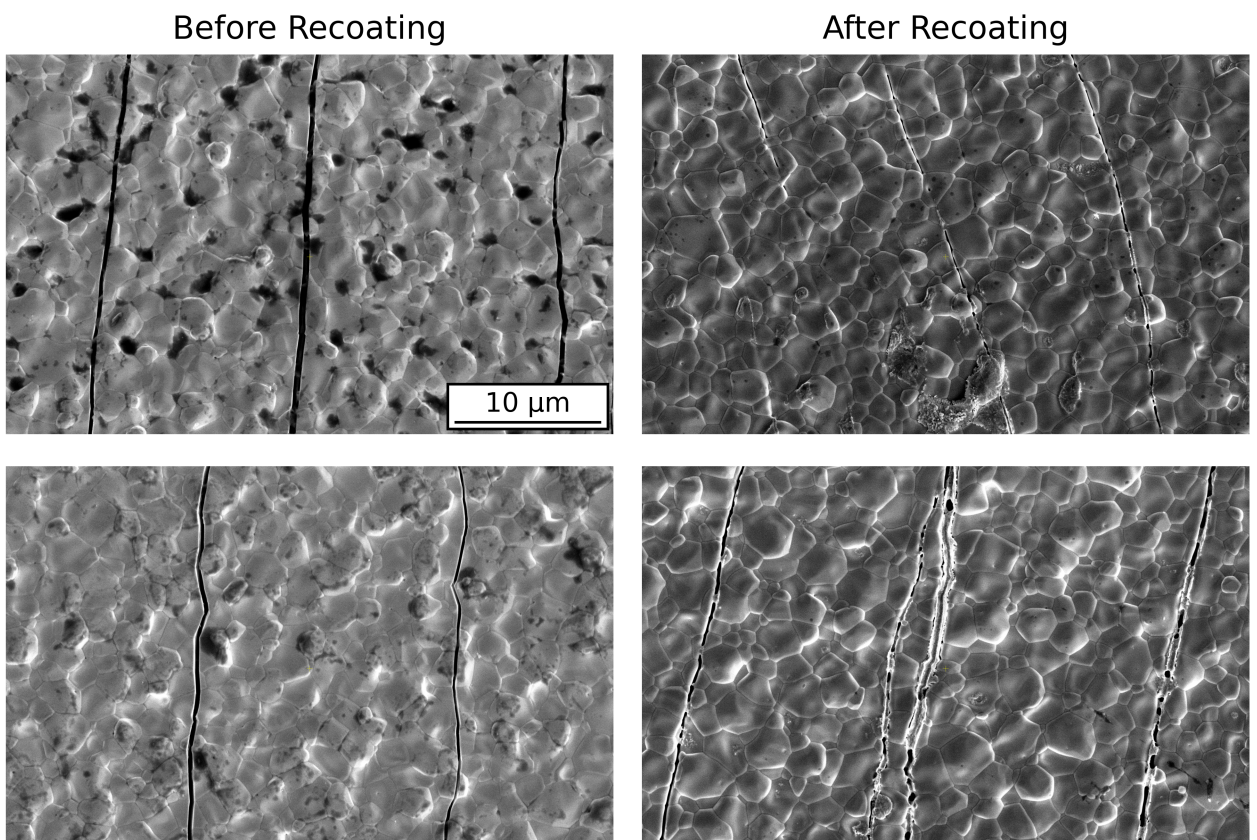


Figure 2.3: This figure shows micrographs of elongated Nb<sub>3</sub>Sn coated wires. The left side shows the samples before treatment with recoating and the right side shows the samples after recoating. After the recoating treatment the cracks appear to be partially filled with new Nb<sub>3</sub>Sn.

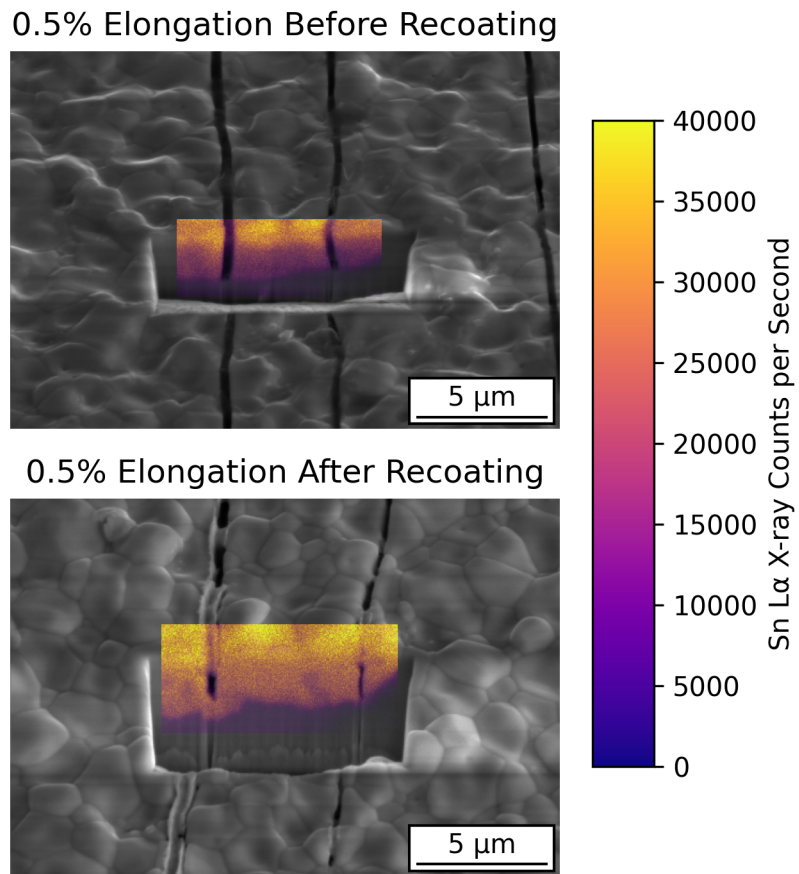


Figure 2.4: The cross section of the film cracks is imaged using FIB/SEM before and after recoating. The Sn content of the cracks is measured qualitatively using Energy dispersive X-ray Spectroscopy (EDS). We find that there is new  $\text{Nb}_3\text{Sn}$  material both in the crack and in the substrate at the base of the crack. There is no evidence of Sn rich phases in the crack.

# Bibliography

- [1] C. Boulware, S. Baurac, J. Diemer, T. Grimm, A. Schnepf, *et al.*, “High-power superconducting electron linacs for commercial applications,” 2019.
- [2] D. B. Liarte, S. Posen, M. K. Transtrum, G. Catelani, M. Liepe, and J. P. Sethna, “Theoretical estimates of maximum fields in superconducting resonant radio frequency cavities: stability theory, disorder, and laminates,” *Superconductor Science and Technology*, vol. 30, no. 3, p. 033002, 2017.
- [3] G. Catelani and J. P. Sethna, “Temperature dependence of the superheating field for superconductors in the high- $\kappa$  london limit,” *Physical Review B*, vol. 78, no. 22, p. 224509, 2008.
- [4] F. P.-J. Lin and A. Gurevich, “Effect of impurities on the superheating field of type-ii superconductors,” *Physical Review B*, vol. 85, no. 5, p. 054513, 2012.
- [5] T. Kubo, “Superfluid flow in disordered superconductors with dynes pair-breaking scattering: Depairing current, kinetic inductance, and superheating field,” *Physical Review Research*, vol. 2, no. 3, p. 033203, 2020.
- [6] J. N. Galayda, “The lcls-ii: A high power upgrade to the lcls,” tech. rep., SLAC National Accelerator Lab., Menlo Park, CA (United States), 2018.
- [7] S. Posen and D. L. Hall, “Nb3sn superconducting radiofrequency cavities: fabrication, results, properties, and prospects,” *Superconductor Science and Technology*, vol. 30, no. 3, p. 033004, 2017.
- [8] U. Pudasaini, G. V. Eremeev, J. W. Angle, J. Tuggle, C. E. Reece, and M. J. Kelley, “Growth of nb3sn coating in tin vapor-diffusion process,” *Journal of Vacuum Science & Technology A*, vol. 37, no. 5, 2019.
- [9] R. Porter, T. Arias, P. Cueva, J. Ding, D. Hall, M. Liepe, D. Muller, N. Sitaraman, *et al.*, “Update on nb3sn progress at cornell university,” *Proc. of IPAC 2018*, 2018.
- [10] G. Eremeev, B. Clemens, K. Macha, H. Park, R. S. Williams, *et al.*, “Development of a nb3sn cavity vapor diffusion deposition system,” in *Proc. SRF*, vol. 13, pp. 603–606, 2013.
- [11] S. Posen, J. Lee, D. N. Seidman, A. Romanenko, B. Tennis, O. Melnychuk, and D. Sergatskov, “Advances in nb3sn superconducting radiofrequency cavities towards first practical accelerator applications,” *Superconductor Science and Technology*, vol. 34, no. 2, p. 025007, 2021.

- [12] J. Knobloch, R. Geng, M. Liepe, H. Padamsee, *et al.*, “High-field q slope in superconducting cavities due to magnetic field enhancement at grain boundaries,” in *Proceedings of the 9th Workshop on RF Superconductivity*, pp. 77–91, Citeseer, 1999.
- [13] C. Xu, C. E. Reece, and M. J. Kelley, “Simulation of nonlinear superconducting rf losses derived from characteristic topography of etched and electropolished niobium surfaces,” *Physical Review Accelerators and Beams*, vol. 19, no. 3, p. 033501, 2016.
- [14] R. Porter, D. L. Hall, M. Liepe, J. Maniscalco, *et al.*, “Surface roughness effect on the performance of nb3sn cavities,” *Proc. of LINAC 2016*, 2016.
- [15] T. Kubo, “Magnetic field enhancement at a pit on the surface of a superconducting accelerating cavity,” *Progress of Theoretical and Experimental Physics*, vol. 2015, no. 7, p. 073G01, 2015.
- [16] U. Pudasaini, G. Eremeev, C. Reece, J. Tuggle, and M. Kelley, “Studies of electropolishing and oxypolishing treated diffusion coated nb3sn surfaces,” in *Proc. 9th Int. Particle Accelerator Conf.(IPAC'18), Vancouver, Canada*, pp. 3954–3957, 2018.
- [17] U. Pudasaini, G. Eremeev, C. E. Reece, J. Tuggle, and M. Kelley, “Post-processing of nb3sn coated niobium,” 2017.
- [18] H. Hu, “Reducing surface roughness of nb3sn through chemical polishing treatments,” in *Conference on RF Superconductivity*, 2019.
- [19] N. S. Sitaraman, M. M. Kelley, R. D. Porter, M. U. Liepe, T. A. Arias, J. Carlson, A. R. Pack, M. K. Transtrum, and R. Sundararaman, “Effect of the density of states at the fermi level on defect free energies and superconductivity: A case study of nb 3 sn,” *Physical Review B*, vol. 103, no. 11, p. 115106, 2021.
- [20] K. Saito, “Development of electropolishing technology for superconducting cavities,” in *Proceedings of the 2003 Particle Accelerator Conference*, vol. 1, pp. 462–466, IEEE, 2003.
- [21] A. C. Crawford, “Extreme diffusion limited electropolishing of niobium radiofrequency cavities,” *Nuclear Instruments and Methods in Physics Research Section A: Accelerators, Spectrometers, Detectors and Associated Equipment*, vol. 849, pp. 5–10, 2017.
- [22] T. Higuchi, S. Noguchi, M. Ono, Y. Funahashi, K. Saitô, H. Inoue, E. Kako, T. Suzuki, and T. Shishido, “Investigation on barrel polishing for superconducting niobium cavities,” tech. rep., SCAN-9605109, 1996.
- [23] C. Cooper and L. Cooley, “Mirror-smooth surfaces and repair of defects in superconducting rf cavities by mechanical polishing,” *Superconductor Science and Technology*, vol. 26, no. 1, p. 015011, 2012.
- [24] C. Cooper, K. Saito, B. Bullock, S. Joshi, and A. Palczewski, “Centrifugal barrel polishing of cavities worldwide,” in *Proceedings of SRF*, pp. 571–575, 2011.
- [25] C. Xu, H. Tian, C. E. Reece, and M. J. Kelley, “Enhanced characterization of niobium surface topography,” *Physical Review Special Topics-Accelerators and Beams*, vol. 14, no. 12, p. 123501, 2011.

- [26] U. Pudasaini, M. Kelley, G. Eremeev, C. Reece, and J. Tuggle, “Surface studies of nb<sub>3</sub>sn coated samples prepared under different coating conditions,” in *Proc. 18th Int. Conf. RF Superconductivity (SRF’17)*, pp. 894–899, 2017.
- [27] A. Palczewski, G. Ciovati, Y. Li, and R. Geng, “Exploration of material removal rate of srf elliptical cavities as a function of media type and cavity shape on niobium and copper using centrifugal barrel polishing (cbp),” tech. rep., Thomas Jefferson National Accelerator Facility (TJNAF), Newport News, VA . . . , 2013.
- [28] Z. Sun, Z. Baraissov, C. A. Dukes, D. K. Dare, T. Oseroff, M. O. Thompson, D. A. Muller, and M. U. Liepe, “Surface oxides, carbides, and impurities on rf superconducting nb and nb<sub>3</sub>sn: A comprehensive analysis,” 2023.
- [29] A. Cano, G. V. Eremeev, J. R. Zuazo, J. Lee, B. Luo, M. Martinello, A. Romanenko, and S. Posen, “Selective thermal evolution of native oxide layer in nb and nb<sub>3</sub>sn-coated srf grade nb: An in-situ angular xps study,” 2023.
- [30] Y. Pischalnikov, R. Carcagno, F. Lewis, R. Nehring, R. Pilipenko, W. Schappert, *et al.*, “Rf control and daq systems for the upgraded vertical test facility at fnal,” 2014.
- [31] P. Kulyavtsev, G. Eremeev, and S. Posen, “Simulations of nb<sub>3</sub>sn layer rf field limits due to thermal impedance,” 2021.
- [32] R. D. Porter, *Advancing the maximum accelerating gradient of niobium-3 tin superconducting radiofrequency accelerator cavities: RF measurements, dynamic temperature mapping, and material growth*. PhD thesis, Cornell University, 2021.
- [33] J. Lee, S. Posen, Z. Mao, Y. Trenikhina, K. He, D. L. Hall, M. Liepe, and D. N. Seidman, “Atomic-scale analyses of nb<sub>3</sub>sn on nb prepared by vapor diffusion for superconducting radiofrequency cavity applications: a correlative study,” *Superconductor Science and Technology*, vol. 32, no. 2, p. 024001, 2018.
- [34] E. Viklund, J. Lee, D. N. Seidman, and S. Posen, “Three-dimensional reconstruction of nb<sub>3</sub>sn films by focused ion beam cross sectional microscopy,” *IEEE Transactions on Applied Superconductivity*, pp. 1–5, 2023.